Astronomy & Astrophysics manuscript no. 3186 February 2, 2008
(DOI: will be inserted by hand later)

On the link between rotation, chromospheric activity and Li abundance in subgiant stars

J. D. do Nascimento Jr.[1], B. L. Canto Martins[1], C. H. F. Melo[2,1], G. Porto de Mello[3] and J. R. De Medeiros[1]

[1] Departamento de Física, Universidade Federal do Rio Grande do Norte, 59072-970 Natal, RN., Brazil
[2] European Southern Observatory, Casilla 19001, Santiago 19, Chile
[3] Observatório do Valongo, Ladeira do Pedro Antonio, 43, 20080-090, Rio de Janeiro, RJ., Brazil

Received / Accepted

Abstract. The connection rotation–CaII emission flux–lithium abundance is analyzed for a sample of bona fide subgiant stars, with evolutionary status determined from HIPPARCOS trigonometric parallax measurements and from the Toulouse–Geneva code. The distribution of rotation and CaII emission flux as a function of effective temperature shows a discontinuity located rather around the same spectral type, F8IV. Blueward of this spectral type subgiants have a large spread of values of rotation and CaII flux, whereas stars redward of F8IV show essentially low rotation and low CaII flux. The strength of these declines depends clearly on stellar mass. The abundance of lithium also shows a sudden decrease. For subgiants with mass lower than about 1.2 $M_\odot$ the decrease is located later than that in rotation and CaII flux, whereas for masses higher than 1.2 $M_\odot$ the decrease in lithium abundance is located around the spectral type F8IV. The discrepancy between the location of the discontinuities of rotation and CaII emission flux and log $n(Li)$ for stars with masses lower than 1.2 $M_\odot$ seems to reflect the sensitivity of these phenomena to the mass of the convective envelope. The drop in rotation, which results mostly from a magnetic braking, requires an increase in the mass of the convective envelope less than that required for the decrease in log $n(Li)$. The location of the discontinuity in log $n(Li)$ for stars with masses higher than 1.2 $M_\odot$, in the same region of the discontinuities in rotation and CaII emission flux, may also be explained by the behavior of the deepening of the convective envelope. The more massive the star is, the earlier is the increase of the convective envelope. In contrast to the relationship between rotation and CaII flux, which is fairly linear, the relationship between lithium abundance and rotation shows no clear tendency toward linear behavior. Similarly, no clear linear trend is observed in the relationship between lithium abundance and CaII flux. In spite of these facts, subgiants with high lithium content also have high rotation and high CaII emission flux.

Key words. stars: activity stars: abundances – stars: rotation – stars: interiors – stars: late-type

1. Introduction

The study of the influence of stellar rotation on chromospheric activity and on the mixing of light elements in evolved stars has undergone some important advances during the past decade. Several authors have reported a rotation-activity relation for evolved stars based on the linear behavior of the chromospheric flux with stellar rotation (e.g.: Rutten 1987; Rutten and Pylyser 1988; Simon and Drake 1989; Strassmeier et al. 1994; Gunn et al. 1998; Pasquini et al. 2000). For a given spectral type, however, a large spread in the rotation–activity relation is observed, which suggests that rotation might not be the only relevant parameter controlling stellar activity. Indeed, results from Pasquini and Brocato (1992) and Pasquini et al. (2000) have shown that chromospheric activity depends on stellar effective temperature and mass.

A possible connection between rotation and abundance of lithium in evolved stars has also been reported in the literature (e.g.: De Medeiros et al. 1997; do Nascimento et al. 2000; De Medeiros et al. 2000). Subgiant and giant stars with enhanced lithium abundance show also enhanced rotation, in spite of a large spread in the abundances of lithium among the slow rotators. In addition, do Nascimento et al. (2000) have pointed to a discontinuity in the distribution of Li abundances as a function of effective temperature later than the discontinuity in rotation (e.g.: De Medeiros and Mayor 1990). Concerning the link between chromospheric activity and light element abundances, Duncan (1981) and Pasquini et al. (1994) have found a clear tendency of solar G–type stars with enhanced CaII surface flux $F(CaII)$ to have a higher

Send offprint requests to: J.D. do Nascimento Jr
Correspondence to: do.nascimento@dfte.ufrn.br

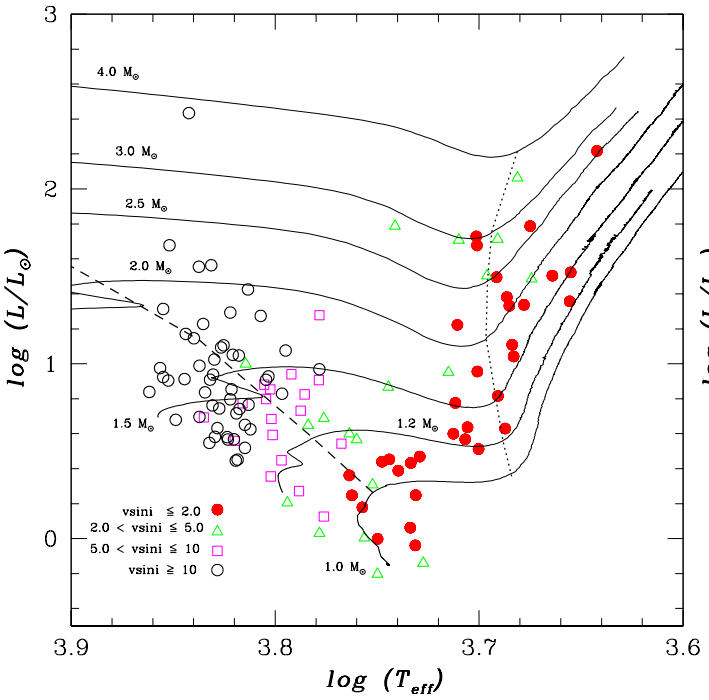

Fig. 1. Distribution of subgiant stars in the HR diagram, with the rotational behavior as a function of luminosity and effective temperature. Luminosities have been derived from the HIPPARCOS parallaxes. Evolutionary tracks at [Fe/H]=0 are shown for stellar masses between 1 and 4 $M_{\odot}$. The dashed line indicates the beginning of the subgiant branch and the dotted line represents the beginning on the red giant branch.

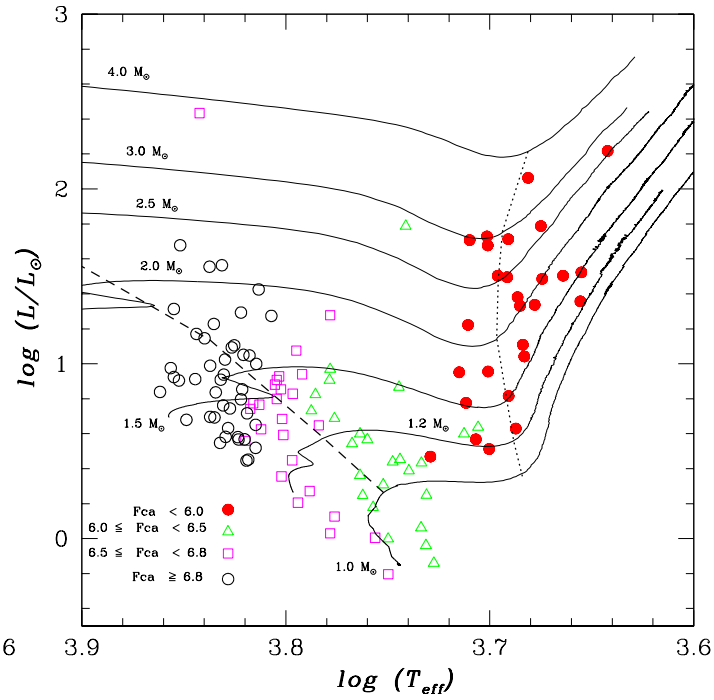

Fig. 2. Distribution of subgiant stars in the HR diagram, with the behavior of the $F(CaII)$ surface flux as a function of luminosity and effective temperature. Luminosities have been derived from the HIPPARCOS parallaxes. Evolutionary tracks are defined as in Fig. 1.

lithium content. This is consistent with the predictions of standard evolutionary models, according to which, activity and abundance of light elements should depend on stellar surface temperature, metallicity and age. In spite of these important studies showing evidence of a connection in between abundance of lithium and rotation and in between chromospheric activity and rotation, in practice, for evolved stars, the mechanisms controlling such connections and their dependence on different stellar parameters like metallicity, mass and age are not yet well established. In this paper, we analyze in parallel the behavior of the chromospheric activity, stellar rotation and lithium abundance along the subgiant branch. In the present approach, the stars are placed in the HR diagram to determine more clearly the location of the discontinuities for these three stellar parameters based on a sample of bona fide subgiants.

2. Working Sample

For this study we have selected a large sample of 121 single stars classified as subgiants in the literature, along the spectral region F, G and K, with rotational velocity, flux of CaII and log $n(Li)$ now available. The rotational velocities $v \sin i$ were taken from De Medeiros and Mayor (1999). By using the CORAVEL spectrometer (Baranne et al. 1979) these authors have determined the projected rotational velocity $v \sin i$ for a large sample of subgiant and giant stars with a precision of about 1 $\mathrm{km\,s^{-1}}$ for stars with $v \sin i$ lower than about 30 $\mathrm{km\,s^{-1}}$. For higher rotators, the estimations indicate an uncertainty of about 10%. The $F(CaII)$ was determined from the CaII H and K line–core emission index S_1 and S_2 listed by Rutten (1987), using the procedure of conversion from the emission index S1 to flux at the stellar surface $F(CaII)$ given by Rutten (1984). The values of log $n(Li)$ were taken from Lèbre et al. (1999) and Randich et al. (1999). Readers are referred to these works for discussion on the observational procedure, data reduction and error analysis. Stellar luminosities were determined as follows. First, the apparent visual magnitudes m_v and trigonometric parallaxes, both taken from HIPPARCOS catalogue (ESA 1997), were combined to yield the absolute visual magnitude M_v. Bolometric correction BC, computed from Flower (1996) calibration, was applied giving the bolometric magnitude which was finally converted into stellar luminosity. The effective temperature was computed using Flower (1996) $(B-V)$ versus T_{eff} calibration. The rotational velocity $v \sin i$, stellar surface flux $F(CaII)$, abundance of lithium log $n(Li)$

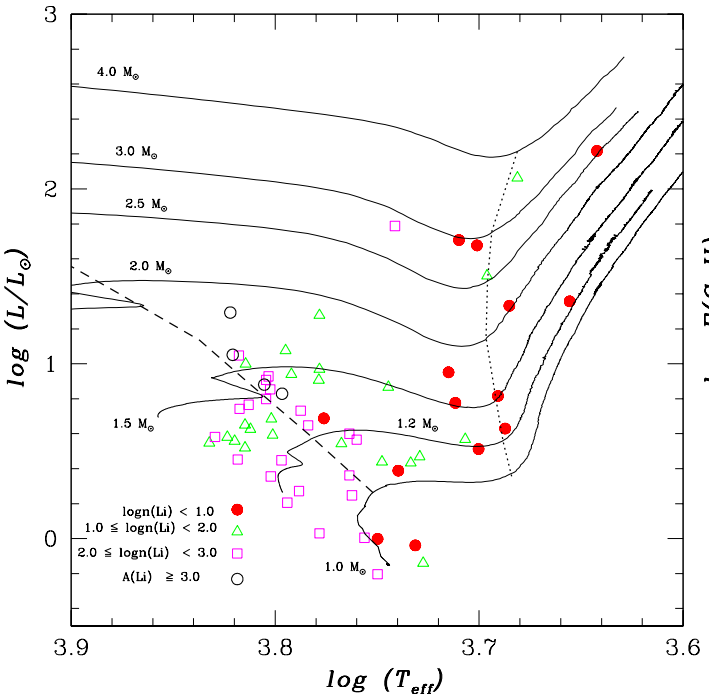

Fig. 3. Distribution of subgiant stars in the HR diagram, with the behavior of Li abundance as a function of luminosity and effective temperature. Luminosities have been derived from the HIPPARCOS parallaxes. Evolutionary tracks are defined as in Fig. 1.

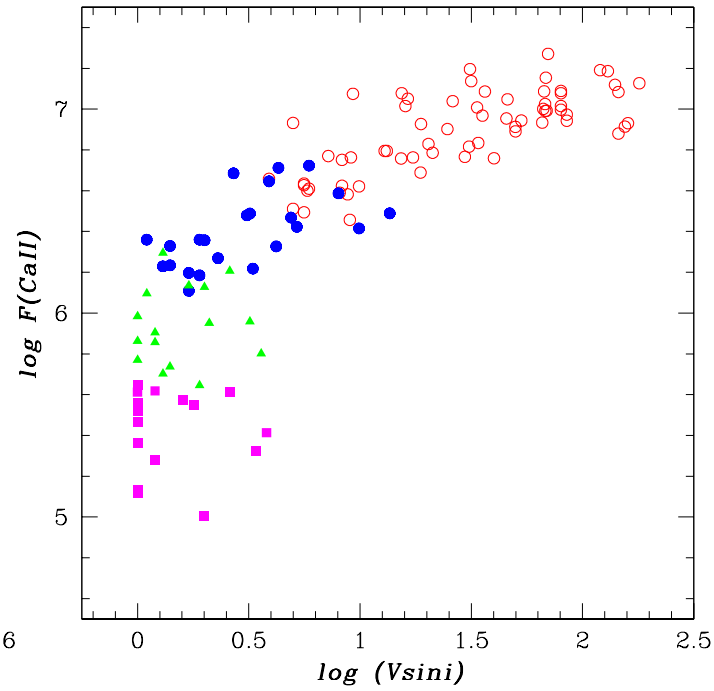

Fig. 4. $log\ F(CaII)$ versus $log(vsini)$ for the program stars. Open circles denote stars with $(B-V) \leq 0.55$, filled circles those with $0.55 < (B-V) \leq 0.75$, triangles stars with $0.75 < (B-V) \leq 0.95$ and squares stars with $(B-V) > 0.95$.

and stellar parameters of the entire sample are presented in Table 1.

3. Results

3.1. The discontinuity in Rotation, CaII emission Flux and Li abundance

As a first step, the stellar luminosity and the effective temperature listed in Table 1 were used to construct the HR diagram to better locate the evolutionary stage of the stars in the sample. In fact, such a procedure seems important because in preceding studies on the link between rotation and chromospheric activity in subgiant stars, only the spectral type was used as a criterion for identifying the stars. Evolutionary tracks were computed from the Toulouse–Geneva code for stellar masses between 1 and 4 $M_{\odot}$, for metallicity consistent with solar–type subgiant stars (see do Nascimento et al 2000 for a more detailed description). Here, in particular, we use the evolutionary tracks computed with solar metallicity because most of the stars in the present sample have $[Fe/H] \sim 0$. The HR diagram with the evolutionary tracks is displayed in Figs. 1, 2 and 3, which in addition show the behavior of the rotational velocity $v \sin i$, surface flux CaII and log $n(Li)$ abundance respectively. In these diagrams the dashed line indicates the evolutionary region where the subgiant branch starts, corresponding to hydrogen exhaustion in stellar central regions, whereas the dotted line represents the beginning of the ascent of the red giant branch. One observes, clearly, that most of the stars in the present sample are effectively subgiants. Nevertheless a small number of stars located in particular on the cool side of the diagrams are rather stars evolving along the red giant branch. In this context, for the purpose of the present analysis, these deviating stars will not be considered as subgiants, in spite of the spectral types assigned in the literature.

Figure 1 shows the well established rotational discontinuity around the spectral type F8IV (e.g.: De Medeiros and Mayor 1990), corresponding to $(B-V) \approx 0.55$ ($\log T_{eff} \sim 3.78$). As shown by these authors, single subgiants blueward of this spectral type show a wide range of rotational velocities from a few km s^{-1} to about one hundred times the solar rotation, whereas subgiants redward of F8IV are essentially slow rotators, except for the synchronized binary systems. Fig. 1 shows clearly that single subgiants redward of the discontinuity with high $v \sin i$ are unusual. The root cause for such a discontinuity seems to be a strong magnetic braking associated with the rapid increase of the moment of inertia, due to evolutionary expansion, once the star evolves along the late F

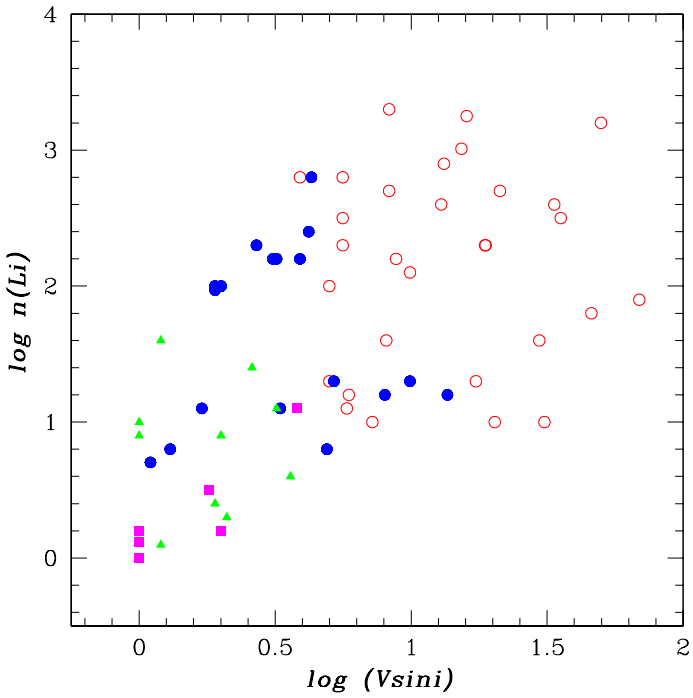

Fig. 5. log $n(Li)$ versus $log(vsini)$ for the program stars. Symbols are defined as in Fig. 4

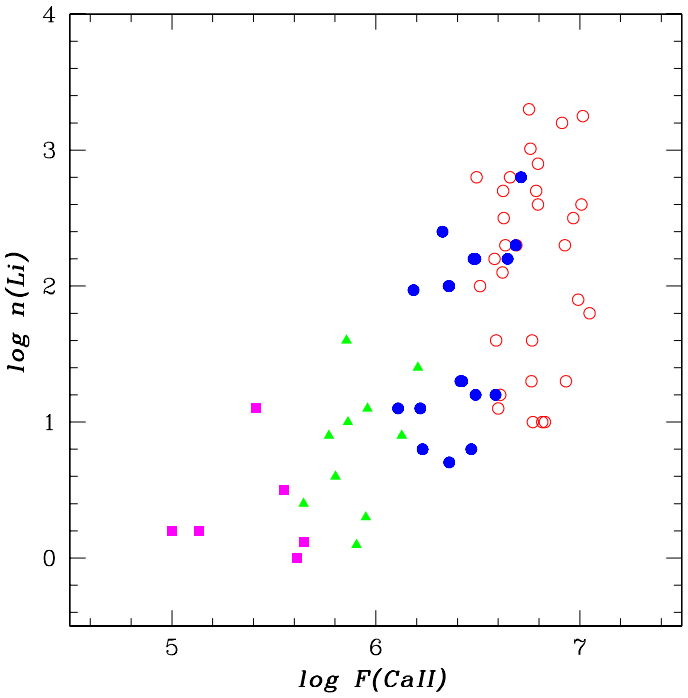

Fig. 6. log $n(Li)$ versus $log\ F(CaII)$ for the program stars. Symbols are defined as in Fig. 4

spectral region (e.g. Gray and Nagar 1985; De Medeiros and Mayor 1990).

Figure 2 shows clear evidence of a discontinuity in the surface flux $F(CaII)$ paralleling the one observed in rotational velocity. In fact, such a sudden decrease in CaII flux of subgiants also parallels that in CIV emission flux found by Simon and Drake (1989). Stars with typical subgiant masses showing the highest CaII flux are located blueward of this discontinuity. Such a drop in the surface chromospheric flux is interpreted by Simon and Drake (1989) as the result of the drop in rotation near the spectral type G0IV. According to these authors, there is a development of a dynamo in late F stars, which induces a strong magnetic braking in a preexisting wind that acts on the outermost layers of the stellar surface. As a consequence the stellar surface will spin down.

Figure 3 shows the behavior of the lithium abundance, with a sudden decrease in log $n(Li)$ for subgiant stars with mass lower than about 1.2 $M_{\odot}$, located a somewhat later than the discontinuity in rotation and in surface $F(CaII)$. Evidence for this decrease in log $n(Li)$ was first pointed out by do Nascimento et al. (2000). According to these authors, such a drop in log $n(Li)$ abundances of subgiants seems to result from the rapid increase of the convective envelope at the late F evolutionary stage. Due to the convective mixing process, Li–rich surface material is diluted towards the stellar interior. For higher masses, the drop in log $n(Li)$ shows a tendency to parallel the discontinuities in $v \sin i$ and $F(CaII)$, near F8IV, corresponding to $(B-V) \approx 0.55$ ($\log T_{eff} \sim 3.78$).

An additional trend is present in Figs. 1 and 2, which show that the fastest rotators and those subgiants with the highest CaII emission flux, namely the stars blueward of F8IV, are mostly stars with mass higher than about 1.2 $M_{\odot}$. Subgiants with mass lower than about 1.2 $M_{\odot}$ show moderate to low rotation as well as moderate to low surface $F(CaII)$. In the region blueward of F8IV, the abundances of lithium show a more complex behavior for stars with masses between 1.2 and 1.5 $M_{\odot}$. Fig. 3 shows a number of stars in this mass interval with low to moderate log $n(Li)$. Such a fact appears to reflect the so-called dip region observed by Boesgaard & Tripicco (1986).

3.2. The relation Rotation – $F(CaII)$ – log $n(Li)$

As a second step of this study we have analyzed the direct relationship between rotation, $F(CaII)$ and log $n(Li)$ for the stars of the sample. Figure 4 shows the surface $F(CaII)$ versus the rotational velocity $v \sin i$, where stars are separated by intervals of $(B-V)$. Stars earlier than the rotational discontinuity, typically those with $(B-V) \leq 0.55$, are represented by open circles, solid circles stand for stars with $0.55 < (B-V) \leq 0.75$, triangles stand for stars with $0.75 < (B-V) \leq 0.95$ and squares represent stars with $(B-V) > 0.95$. The well established correlation between rotation and chromospheric emission flux (e.g. Simon and Drake 1989), here represented by the

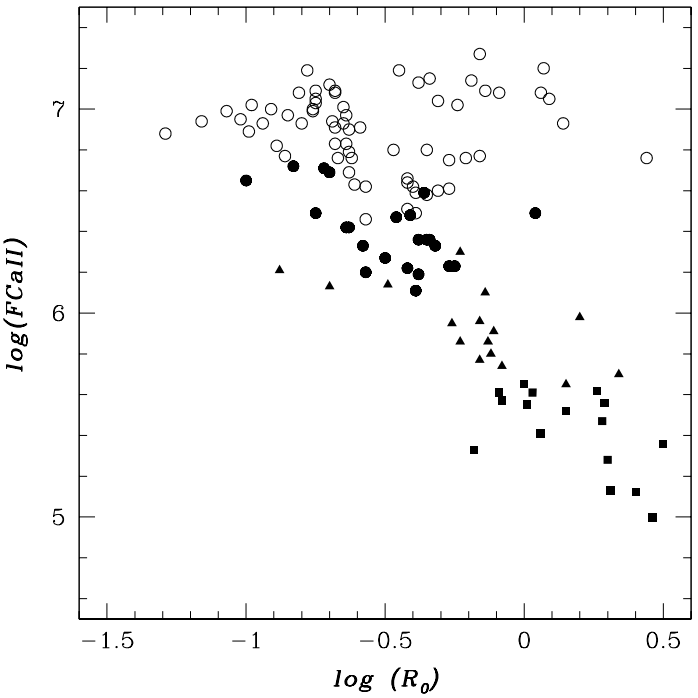

Fig. 7. The $F(CaII)$ versus the Rossby number R_0. The Symbols are defined as in Fig. 4.

surface $F(CaII)$, is clearly confirmed for the present sample of bona fide subgiants.

Figure 5 presents the behavior of log $n(Li)$ as a function of the rotational velocity $v \sin i$, confirming the trend of a fair connection in between abundance of Li and $v \sin i$ in subgiant stars already observed by other authors (e.g. De Medeiros et al. 1997).

Finally, Fig. 6 shows the surface $F(CaII)$ as a function of log $n(Li)$. In spite of more a limited number of stars than in Figs. 4 and 5, we observe a trend for a connection between $F(CaII)$ and log $n(Li)$ following rather the behavior observed in the $v \sin i$ versus log $n(Li)$ relation.

3.3. The connection $F(CaII)$ emission flux–Rossby number

A close examination of the rotation versus $F(CaII)$ relation presented in Fig. 4 shows that the amount by which it deviates from a linear correlation depends on the (B–V) color interval. A similar color dependence was observed by Noyes et al. (1984), who removed such an effect by introducing the dimensionless Rossby number $R_0 = P_{\rm rot}/\tau_{\rm conv}$, as a mesure of the rotational velocity. This dependence was also noted by Simon and Drake (1989) for subgiant stars, by analysing the relation $F(CIV)$ versus rotation. These results confirm that rotation is not the only parameter expected to influence stellar chromospheric activity; another is the stellar mass, or equivalently, the position of the star in the HR diagram, which dictates the properties of the stellar convective zone. The deepening of the convective zone, or its convective turnover time is, in particular, expected to play a relevant role in the dynamo generation. The Rossby number, in fact, determines the extent to which rotation can induce both helicity and differential rotation required for dynamo activity in the convective zone. To analyse the connection $F(CaII)$ emission flux–Rossby number, we have computed R_0 for all the stars of the present sample. The convective turnover time $\tau_{\rm conv}$ was estimated from the iterated function in (B–V) given by Noyes et al. (1984), whereas the rotation period was estimated indirectly from the $v \sin i$ given in Table 1. A statistical correction of $\pi/4$ was taken in consideration, to compensate for $\sin i$ effects. The stellar radii were estimated following the standard expression as a function of effective temperature and luminosity. Figure 7 presents the behavior of $F(CaII)$ as a function of the Rossby number R_0, with two clear different features. For stars with $(B-V) > 0.55$ the correlation of chromospheric activity, given by $F(CaII)$, with R_0 is significantly better than with rotational velocity, whereas stars with $(B-V) \leq 0.55$ show $F(CaII)$ rather uniformly high and independent of the R_0. A similar result was found by Simon and Drake (1989), by analysing the $F(CIV)$ versus R_0 relation.

3.4. The behavior of log $n(Li)$ as a function of the deepening of the convective envelope

The level of dilution of lithium depends strongly on the level of convection. In this context it sounds interesting to analyse the behavior of lithium abundance as a function of the deepening of the convective zone for the present sample of stars. For this purpose we have estimated the mass of each star M_* from the HR diagram presented in Sec. 3.1 and then estimated the mass of the convective zone M_{CZ} from an iterated function M_{CZ} (M_*, Teff) constructed on the basis of the study by do Nascimento et al. (2000) on the deepening (in mass) of the convective envelope of evolved stars. These authors present the behavior of M_{CZ} as a function of Teff for stars with masses between 1.0 and 4.0 $M_\odot$. Figure 8 shows the behavior of log $n(Li)$ in the M_{CZ}/M_* versus Teff diagram. It is clear that most of the stars with high lithium content present an undeveloped convective envelope, whereas stars with low log $n(Li)$ have a developed convective envelope.

4. Discussion

At this point we can inquire about the root cause of the apparent discrepancy in the location of the discontinuities in $v \sin i$ and $F(CaII)$ and that for log $n(Li)$. In fact, should one expect, from the evolutionary point of view, that the discontinuity in log $n(Li)$ follows the one in $v \sin i$ as well as that in $F(CaII)$? First of all, let us recall that in the specific case of late–type evolved stars, chromospheric activity reflects the presence of magnetic fields which are relevant for the heating of the chromosphere as

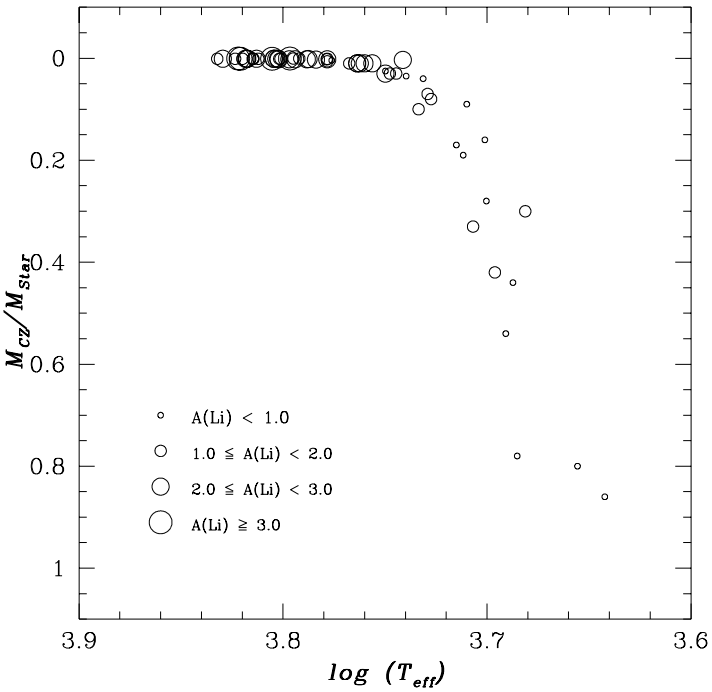

Fig. 8. The deepening (in mass) of the convective envelope as a function of the effective temperature for the stars in the present sample. The symbol size is proportional to the Li abundances quoted in.

well as for mass and angular momentum losses. The intensity and spatial distribution of magnetic fields are very probably determined by a dynamo process, whose mode of operation and efficiency depends on the interplay between stellar rotation and subphotospheric convective motions. In this context one should expect a direct link between the discontinuities in $v \sin i$ and $F(CaII)$, with a drop at the same spectral region, if chromospheric activity is directly controlled by rotation. As shown by Fig. 7, this is true, in particular, for stars located redward of the spectral region of the discontinuity.

The question now turns to the apparent discrepancy in the location of the discontinuity in log $n(Li)$ in relation to the location of the discontinuities in $v \sin i$ and $F(CaII)$ for subgiant stars with masses lower than about 1.2 $M_{\odot}$. This discrepancy can be understood as a result of the sensitivity of these phenomena to the mass of the convective envelope. In the case of the rotational discontinuity, a small increase in the mass of the convective envelope is enough to turn the dynamo on. This same dynamo will be responsible to the magnetic braking causing a drop in the rotation rate and the consequent shutdown of the dynamo itself. Later, the convective envelope will continue to deep reaching a region previously devoid of Li. At this point, the Li brought from the surface layers is diluted and its abundance drops. This fact explains clearly the discrepancy between the location of the discontinuity in log $n(Li)$ in relation to the one for $vsini$ and $F(CaII)$, as observed from Figs. 1 to 3. The fact that a magnetic braking might operate with very small changes in the mass of the convective envelope is further reinforced by the location of the discontinuity in the $F(CaII)$ flux at the late F spectral region. Previous studies (e.g.: do Nascimento et al. 2000) show that the development of the convective envelope towards the stellar interior starts at this spectral region, reaching a maximum within the middle to late G spectral region. In short, the drop in $v \sin i$ and $F(CaII)$ is earlier than that in log $n(Li)$ because, in contrast to the former, this latter requires a large increase in the mass of the convective envelope. Figure 8 shows that Li dilution increases abruptly with the deepening of the convective envelope. In fact, the observed discontinuity in log $n(Li)$ seems to be controlled directly by the increasing of the deepening of the convective envelope.

The observed trend for a same location, of the discontinuities in $v \sin i$ and log $n(Li)$ for stars with masses larger than about 1.2 $M_{\odot}$ may also be explained by following the behavior of the deepening of the convective envelope. As shown by do Nascimento et al. (2000, see their Fig. 4), the changes in the mass of the convective envelope at a given effective temperature in the range from $\log T_{eff} \sim 3.75$ to $\log T_{eff} \sim 3.68$, are more important for stars with masses in the increasing sequence of masses from 1.0 $M_{\odot}$ to 2.5 $M_{\odot}$. The more massive the star is, in this range of masses, the earlier is the increasing of the convective envelope. In this context, a sudden decrease in log $n(Li)$ of stars with masses larger than about 1.2 $M_{\odot}$, paralleling the rotational discontinuity, should be expected.

The relationship between $v \sin i$ and surface $F(CaII)$, as presented in Fig. 4, confirms the results found by other authors for subgiant stars (e.g.: Strassmeier et al. 1994) and for other luminosity classes (Strassmeier et al. 1994; Pasquini et al. 2000). In addition, one observes a trend of increasing scattering in the $v \sin i$ versus $F(CaII)$ relation, confirming previous claims that rotation might not be the only relevant parameter controlling chromospheric activity. In this context, Pasquini et al. (2000) have found for giant stars a clear dependence of $F(CaII)$ flux with a high power of stellar effective temperature, whereas Strassmeier et al. (1994) have found that the CaII flux from the cooler evolved stars depends more strongly upon rotation than the CaII flux from the hotter evolved stars. The behavior of $F(CaII)$ as a function of the Rossby number R_0, presented in Fig. 7, shows two clear trends: For stars with (B–V) larger than about 0.55 the $F(CaII)$ tends towards a linear correlation with R_0; stars with (B–V) lower than about 0.55 show $F(CaII)$ rather uniformly high and independent of R_0, pointing for a component of chromospheric activity independent of rotation. Different authors (e.g.: Wolff et al. 1986) suggest that the chromospheres of early F stars may be heated by the shock dissipation of sound waves, rather than by the dynamo process that control the chromospheric activity in G– and K–type stars.

The dependence of lithium abundance upon rotation observed in Fig. 5 exists in the sense that the fastest rotators also have the highest lithium content. Nevertheless, there is no clear linear relation between these two parameters. Fig. 5 also shows a large spread in the Li content at a given $v \sin i$ value, covering at least 2 magnitudes in log $n(Li)$. Such a spread shows a clear tendency to increase with rotation and effective temperature. For $v \sin i$ lower than about 10 km s^{-1}, in particular, the log $n(Li)$ values range from about 0.0 to about 3.0. Such a spread was also observed by De Medeiros et al. (1997) and do Nascimento et al. (2000). Finally, the behavior of log $n(Li)$ as a function of CaII emission flux presented in Fig. 6 seems to follow roughly the same trend observed for the relation $v \sin i$ versus log $n(Li)$. Subgiants with high lithium content also show high $F(CaII)$, but there is no clear linear relation between these two parameters.

5. Summary and conclusions

In the search for a better understanding of the influence of stellar rotation on chromospheric activity and lithium dilution, we have analyzed the relationship rotation–CaII emission flux–Li abundance along the subgiant branch, on the basis of a sample of bona fide subgiants, reclassified from HIPPARCOS data. The evolutionary status of all the stars was determined from trigonometric parallax taken from this data base and evolutionary tracks computed from the Geneva–Toulouse code. The distributions of the rotational velocity and of the CaII emission flux show similar behavior. For both parameters we observe a sudden decrease around the spectral type F8IV, confirming previous studies. Nevertheless, the extent of these discontinuities depends on the stellar mass. Stars with masses around 1.5 M$_\odot$ show a more important decrease in rotation and CaII emission flux, than stars with masses lower than about 1.2 M$_\odot$. Clearly, stars blueward of F8IV, with masses higher than 1.2 M$_\odot$, rotate faster and are more active than those with masses lower than about 1.2 M$_\odot$. The distribution of Li abundance versus effective temperature, in spite of a sudden decrease in the late–F region shows a trend for a more complex behavior. First, stars with masses lower than about 1.2 M$_\odot$ show a discontinuity in log $n(Li)$ somewhat later than the discontinuities in rotation and CaII emission flux, whereas stars with higher masses present a decline in log $n(Li)$ rather around the spectral type F8IV. In addition, a group of stars blueward of F8IV with masses between 1.2 and 1.5 M$_\odot$ shows moderate to low log $n(Li)$, which seems to reflect the effects of the so-called Boesgaard–Tipico dip region. The discrepancy in the location of the discontinuities of rotation–CaII emission flux and log $n(Li)$ for stars with masses lower than 1.2 M$_\odot$, seems to be the result of the sensitivity of these phenomena to the mass of the convective envelope. The drop in rotation, resulting mostly from a magnetic braking, requires an increase in the mass of the convective envelope less than that required for the sudden decrease in log $n(Li)$, this later resulting from the dilution due to the rapid increase of the convective envelope. The location of the discontinuity in log $n(Li)$ for stars with masses higher than 1.2 M$_\odot$, in the same region of the discontinuities in rotation and CaII emission flux, may also be explained by following the behavior of the deepening of the convective envelope. The more massive the star is, the earlier is the increase of the convective envelope. The present work confirms that the dilution of Li depends strongly on the deepening of the convective envelope.

The relationship between rotation and CaII emission flux confirms previous results found by other authors. CaII emission flux shows a correlation with rotation. Nevertheless, the large spread in the CaII flux–$v \sin i$ relation reinforces previous suggestions that rotation might not be the only relevant parameter controlling stellar chromospheric activity. In fact, the relation $F(CaII)$ versus Rossby number confirms that chromospheric activity of subgiant stars with (B–V) larger than about 0.55 depends rather linearly on rotation, whereas for stars with (B–V) lower than about 0.55 activity is rather independent of rotation. The relationship between log $n(Li)$ and rotation shows a behavior less clear than that between CaII flux and rotation. Of course the present study confirms a dependence of lithium abundance upon rotation, in the sense that stars with the high rotation have also high lithium content. In spite of this fact, there is no clear linear relationship between these two parameters, with a spread more important than that observed in the $F(CaII)$ –$v \sin i$ relation. The behavior of the relationship between lithium abundance and CaII emission flux seems to follow that observed for log $n(Li)$–$v \sin i$. Stars with the high activity also show high lithium content. In both cases there is a remarkable increase in scattering in the log $n(Li)$–$v \sin i$ and log $n(Li)$–CaII flux relations with increasing $v \sin i$ and CaII flux, respectively. Such a fact appears to indicate that the influence of rotation on stellar activity is greater than on lithium dilution. Finally, the present study point to a pressing need for new measurements of chromospheric emission flux and lithium abundance for an homogeneous and larger sample of bona fide subgiant stars, with a larger range of metallicities, than that analyzed here. With these additional data it will be possible to analyze the influence of rotation upon activity and lithium dilution on a more solid basis, taking into account the stellar age and metallicity.

Acknowledgements. This work has been supported by continuous grants from the CNPq Brazilian Agency. J.D.N.Jr. acknowledges the CNPq grant PROFIX 540461/01-6. Special thanks to the referee, Dr. R. Cayrel for very useful comments, which greatly improved the quality of this paper.

References

Baranne, A., Mayor, M., Poncet, J. L. 1979, Vistas Astron. 23, 279

Boesgaard, A. M., Trippico, M. J. 1986, ApJ 302, L49

De Medeiros, J. R., Mayor, M. 1990, Cool stars, stellar systems, and the sun; Proceedings of the 6th Cambridge Workshop, Seattle, Astronomical Society of the Pacific, 6, 404

De Medeiros, J. R., do Nascimento, J. D., Jr., Mayor, M. 1997, A&A 317, 701
De Medeiros, J. R., Mayor, M. 1999, A&AS 139, 433
De Medeiros, J. R., do Nascimento, J. D. Jr., Sankarankutty, S., Costa, J. M., Maia, M. R. G. 2000, A&A 363, 239
do Nascimento, J. D. Jr., Charbonnel, C., Lèbre, A., de Laverny, P., De Medeiros, J. R. 2000, A&A 357, 931
Duncan, D.K. 1981, ApJ 248, 651
ESA 1997, The Hipparcos and Tycho Catalogues, ESA SP-1200
Flower, P. J. 1996, ApJ 469, 355
Gray, D. F., Nagar, P. 1985, ApJ 298, 756
Gunn, A. G., Mitrou, C. K., Doyle, J. G. 1998, MNRAS 296, 150
Lèbre, A., de Laverny, P., De Medeiros, J. R., Charbonnel, C., da Silva, L. 1999, A&A 345, 936
Noyes, R. W., Hartmann, L. W., Baliunas, S. L., Duncan, D. K., Vaughan, A. H. 1984, ApJ, 279, 763
Pasquini, L., Brocato, E. 1992, A&A 266, 340
Pasquini, L., Liu, Q., Pallavicini, R. 1994, A&A 287, 191
Pasquini, L., De Medeiros, J. R., Girardi, L. 2000, A&A 361, 1011
Randich, S., Gratton, R., Pallavicini, R., Pasquini, L., Carretta, E. 1999, A&A 348, 487
Rutten, R. G. M. 1984, A&A 130, 353
Rutten, R. G. M. 1987, A&A 177, 131
Rutten, R. G. M., Pylyser, E. 1988, A&A 191, 227
Simon, T., Drake, S., A. 1989, ApJ 346, 303
Strassmeier, K. G., Handler, G., Paunzen, E., Rauth, M. 1994, A&A 281, 855
Uesugi, A., Fukuda, I., 1982, Catalogue of stellar rotational velocities (revised)
Wollf, S. C., Boesgaard, A. M., Simon, T. 1986, ApJ 310, 360

Table 1. The stars of the present workimg sample with their physical parameters

HD	ST	log(L/Lo)	T_{eff}	$v \sin i$	$F(CaII)$	log $n(Li)$
400	F8IV	0.45	6265	5.6	6.635	2.30[a]
645	K0IV	1.33	4844	1.8	5.551	0.50[a]
905	F0IV	0.68	7059	31.6	7.137	
3229	F5IV	1.00	6524	5.0	6.932	1.30[a]
4744	G8IV	1.49	4724	3.4	5.326	
4813	F7IV-V	0.21	6223	3.9	6.658	2.80[a]
5268	G5IV	1.68	5024	1.9	5.646	0.40[a]
5286	K1IV	1.04	4821	1.6	5.573	
6301	F7IV-V	0.65	6528	20.3	6.829	1.00[a]
6680	F5IV	0.63	6735	36.4	7.086	
8799	F5IV	0.85	6628	65.9	6.934	
9562	G2IV	0.57	5755	4.2	6.327	2.40[a]
11151	F5IV	0.80	6637	34.0	6.834	
12235	G2IV	0.54	5855	5.2	6.423	1.30[a]
13421	G0IV	0.91	6006	9.9	6.415	1.30[a]
13871	F6IV-V	0.77	6546	9.1	6.763	
16141	G5IV	0.31	5653	2.3	6.269	
18262	F7IV	0.80	6375	9.9	6.621	2.10[b]
18404	F5IV	0.57	6656	24.7	6.902	
20618	G8IV	1.22	5137	1.0	5.984	
23249	K0IV	0.51	5015	1.0	5.770	0.90[b]
25621	F6IV	0.83	6261	15.3	6.758	3.01[b]
26913	G5IV	-0.20	5621	3.9	6.646	2.20[a]
26923	G0IV	0.03	6002	4.3	6.712	2.80[a]
29859	F7IV-V	0.83	6103	9.0	6.457	
30912	F2IV	1.56	6877	155[f]	6.914	
33021	G1IV	0.36	5803	2.0	6.357	2.00[a]
34180	F0IV	0.74	6721	80[f]	7.015	
34411	G2IV-V	0.25	5785	1.9	6.360	2.00[a]
37788	F0IV	0.92	7160	31.2	7.196	
39881	G5IV	0.18	5718	1.4	6.329	
43386	F5IV-V	0.45	6582	18.8	6.927	2.30[b]
53329	G8IV	1.73	5028	1.3	5.702	
57749	F3IV	2.43	6955	40[f]	6.759	
60532	F6IV	0.94	6195	8.1	6.590	1.60[a]
64685	F2IV	0.70	6873	67.2	7.087	
66011	G0IV	0.97	6002	13.6	6.489	1.20[a]
71952	K0IV	1.11	4828	1.0	5.520	
73017	G8IV	1.50	4915	1.2	5.618	
73593	G0IV	1.38	4857	1.0	5.561	
76291	K1IV	1.50	4614	1.2	5.282	
78154	F7IV-V	0.59	6328	5.8	6.600	1.10[a]
81937	F0IV	1.15	6916	145[f]	7.084	
82074	G6IV	0.95	5188	2.1	5.951	0.30[a]
82328	F6IV	0.88	6388	8.3	6.751	3.30[a]
82734	K0IV	2.06	4800	3.8	5.413	1.10[a]
84117	F9IV	0.27	6142	5.6	6.627	2.50[b]
89449	F6IV	0.63	6488	17.3	6.763	1.30[a]
92588	K1IV	0.57	5091	1.0	5.863	1.00[a]
94386	K3IV	1.36	4525	1.0	5.133	0.20[a]
99028	F2IV	1.05	6619	16.0	7.015	3.25[b]
99329	F3IV	0.91	6989	130[f]	7.186	
99491	K0IV	-0.14	5338	2.6	6.206	1.40[a]

Sources: a – Lèbre et al. (1999); b – De Medeiros et al. (1997); c – Randich et al. (1999); f –Uesugi and Fukuda (1982);

Table 1. Continued. The stars of the present workimg sample with their physical parameters

HD	ST	log(L/Lo)	T_{eff}	$v \sin i$	$F(CaII)$	log $n(Li)$
104055	K2IV	2.22	4388	2.0	5.003	0.20[a]
104304	K0IV	-0.04	5387	2.0	6.127	0.90[a]
105678	F6IV	1.08	6236	29.6	6.766	1.60[a]
107326	F0IV	0.98	7185	120[f]	7.191	
110834	F6IV	1.27	6414	145[f]	6.880	
117361	F0IV	1.09	6707	85[f]	6.973	
119992	F7IV-V	0.36	6341	8.3	6.624	2.70[a]
121146	K2IV	1.52	4520	1.0	5.116	
123255	F2IV	1.17	6980	140[f]	7.119	
124570	F6IV	0.73	6130	5.6	6.494	2.80[a]
125111	F2IV	0.69	6839	9.3	7.075	
125184	G5IV	0.39	5491	1.3	6.229	0.80[a]
125451	F5IV	0.55	6796	46.0	7.048	1.80[a]
125538	G9IV	1.79	4731	1.0	5.363	
126943	F1IV	0.99	6873	80[f]	7.078	
127243	G3IV	1.71	5128	3.6	5.802	0.60[a]
127739	F2IV	0.94	6768	68.0	6.991	
127821	F4IV	0.45	6596	45.5	6.954	
130945	F7IVw	0.93	6358	18.7	6.689	2.30[b]
133484	F6IV	0.77	6502	21.2	6.786	2.70[a]
136064	F9IV	0.65	6079	5.0	6.511	2.00[a]
143584	F0IV	0.84	7273	70[f]	7.271	
145148	K0IV	0.63	4867	1.0	5.612	0.00[c]
150012	F5IV	1.05	6573	35.5	6.968	2.50[a]
154160	G5IV	0.47	5360	1.2	5.856	1.60[a]
154417	F8.5IV-V	0.13	5972	5.9	6.723	
156697	F0-2IV-Vn	1.56	6782	160[f]	6.931	
156846	G3IV	0.69	5972	4.9	6.468	0.80[a]
157347	G5IV	0.00	5621	1.1	6.360	0.70[c]
157853	F8IV	1.79	5511	3.2	6.488	2.20[a]
158170	F5IV	1.28	6002	8.0	6.587	1.20[a]
161797	G5IV	0.43	5414	1.7	6.109	1.10[a]
162003	F5IV-V	0.74	6569	12.9	6.795	2.60[a]
162076	G5IV	1.50	4967	3.2	5.959	1.10[a]
162917	F4IV-V	0.57	6610	50[f]	6.891	
164259	F2IV	0.76	6772	80[f]	6.997	
165438	K1IV	0.82	4907	1.0	5.647	0.12[c]
173949	G7IV	1.71	4909	2.6	5.614	
176095	F5IV	0.91	6375	13.2	6.795	2.90[a]
182572	G8IV	0.25	5384	1.7	6.135	
182640	F0IV	0.90	7119	68.4	7.154	
184663	F6IV	0.58	6660	69.0	6.992	1.90[b]
185124	F3IV	0.72	6592	85[f]	6.943	
188512	G8IV	0.78	5148	1.2	5.905	0.10[c]
190360	G6IV+M6V	0.06	5417	1.7	6.197	
190771	G5IV	0.01	5705	2.7	6.685	2.30[a]
191026	K0IV	0.60	5160	1.3	6.295	
191570	F5IV	0.58	6754	33.6	7.008	2.60[a]
192344	G4IV	0.45	5547	1.4	6.234	
195564	G2.5IV	0.44	5593	1.9	6.185	1.97[c]
196755	G5IV+K2IV	0.87	5553	3.3	6.218	1.10[a]
197373	F6IV	0.52	6528	30.9	6.816	1.00[a]
197964	K1IV	1.34	4764	1.0	5.466	

Sources: a – Lèbre et al. (1999); b – De Medeiros et al. (1997); c – Randich et al. (1999); f –Uesugi and Fukuda (1982);

Table 1. Continued. The stars of the present workimg sample with their physical parameters

HD	ST	log(L/Lo)	T_{eff}	$v \sin i$	$F(CaII)$	log $n(Li)$
198149	K0IV	0.96	5022	1.4	5.737	
201507	F5IV	1.23	6844	16.4	7.051	
201636	F3IV	0.91	6791	67.9	7.025	
202444	F1IV	1.02	6758	26.1	7.039	
202582	G2IV+G2IV	0.60	5803	3.1	6.479	2.20[a]
205852	F1IV	1.68	7109	180[f]	7.127	
207978	F6IV-Vvw	0.56	6605	7.2	6.770	1.00[a]
208703	F5IV	0.84	6829	15.4	7.078	
210210	F1IV	1.31	7160	80[f]	7.089	
212487	F5IV	0.85	6345	8.8	6.582	2.20[b]
216385	F7IV	0.68	6336	5.9	6.610	1.20[a]
218101	G8IV	0.64	5078	1.1	6.096	
219291	F6IVw	1.43	6506	53.1	6.944	
223421	F2IV	1.11	6688	66.6	7.001	
224617	F4IV	1.29	6637	49.9	6.913	3.20[b]

Sources: a – Lèbre et al. (1999); b – De Medeiros et al. (1997); c – Randich et al. (1999); f –Uesugi and Fukuda (1982);